A Guide to WSR-88D Data Quality Phenomena and Anomalies

Amy E. Daniel
Operations Branch

Radar Operations Center
Norman, OK 73069
June 2020

Over the years there have been numerous items of interest observed in WSR-88D data. This document contains examples and brief discussions of many of these items, which are listed below. A list of acronyms is available on the last page.

Current WSR-88D Topics
Biological Targets
Bird/Bat Signatures
Chaff
CMD False Alarms
Data Voids from Bypass Map
Earthquakes
Exclusion Zone Holes
PHI Wrapping
Popcorn Cities
QPE Ring/Discontinuity
Sea Spray
Sidelobe Contamination: Horizontal
Sidelobe Contamination: Vertical
Start of Elevation Discontinuity
Stripes in SRM
Terrain Spikes & Clutter Bursts
Three Body Scatter Spike
Velocity Dealiasing Errors: VCP 31
Velocity Dealiasing Errors
Wet Radome
ZDR Wedges/Spikes

Past WSR-88D Topics
Clutter Footprint
PHI Initial Target Value
Radial Spikes of Zero Knots in SW
Shimmy
SZ-2 in Manual PRF Bug

Current Topics:

Biological Targets

It is rather common, especially in the warm season, to see numerous biological targets (i.e., insects, birds, and even vegetation on radar displays. These radar returns can be quite strong, exceeding 30, sometimes 40 dBZ. In addition to relatively high R values, ZDR values will often also be high while CC values will be low. The addition of Dual Pol variables allows us to confirm that the strong R returns are non-meteorological.

A video at http://www.npr.org/sections/krulwich/2011/06/01/128389587/look-up-the-billion-bug-highway-you-cant-see discusses just how many insects can be within a 0.6-mile column of air.

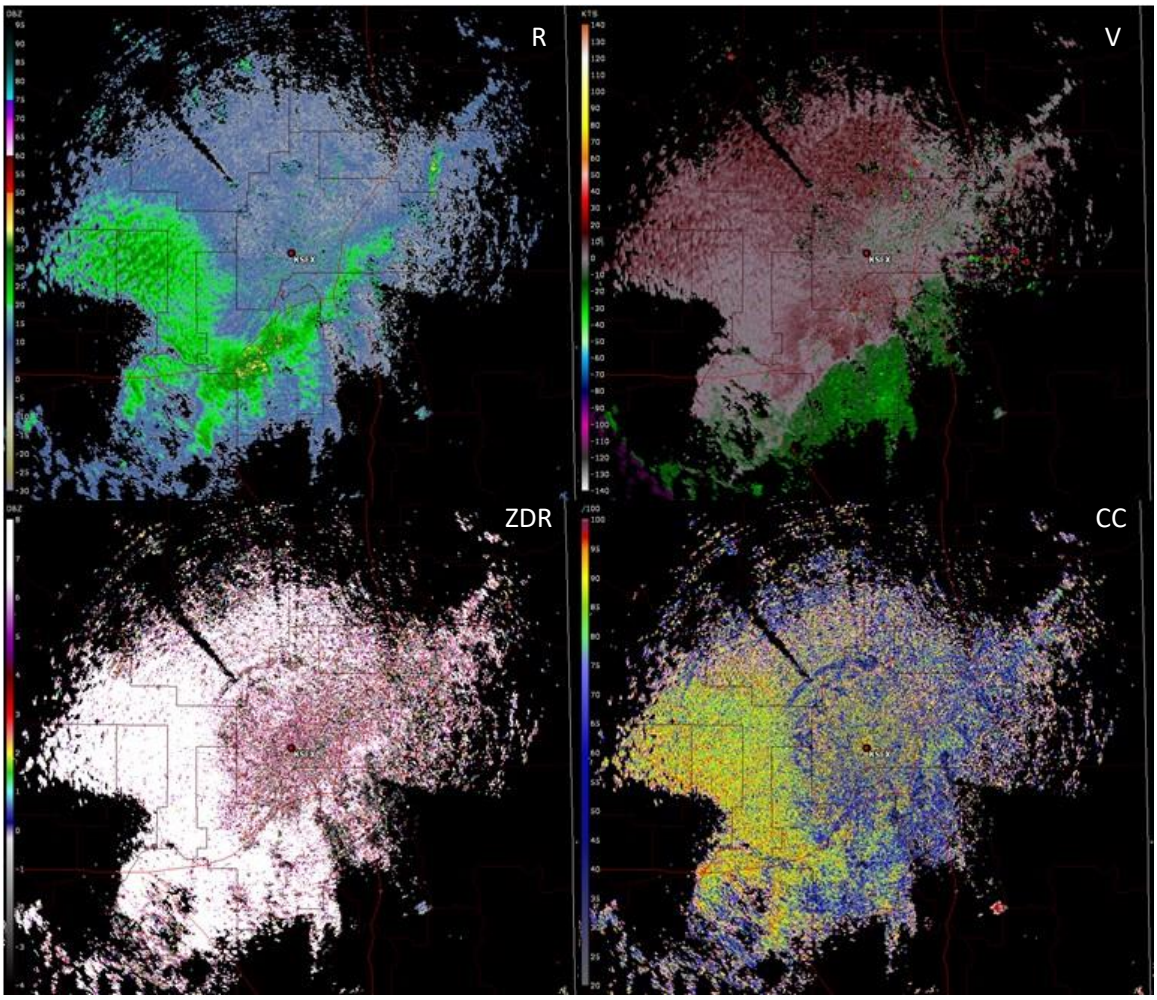

Bird & Bat Signatures

Other examples of detecting biological targets include bird and bat signatures. Birds are often seen flying away from their nesting grounds near sunrise while bats are seen flying away from their caves near sunset. The returns often start out in a circular appearance and then break apart as the animals change their course. They often show divergent velocity signatures. Dual-Pol variables simply add to the confirmation that these returns are biological. ZDR estimates are often high while CC estimates are often low. A bird example is shown below.

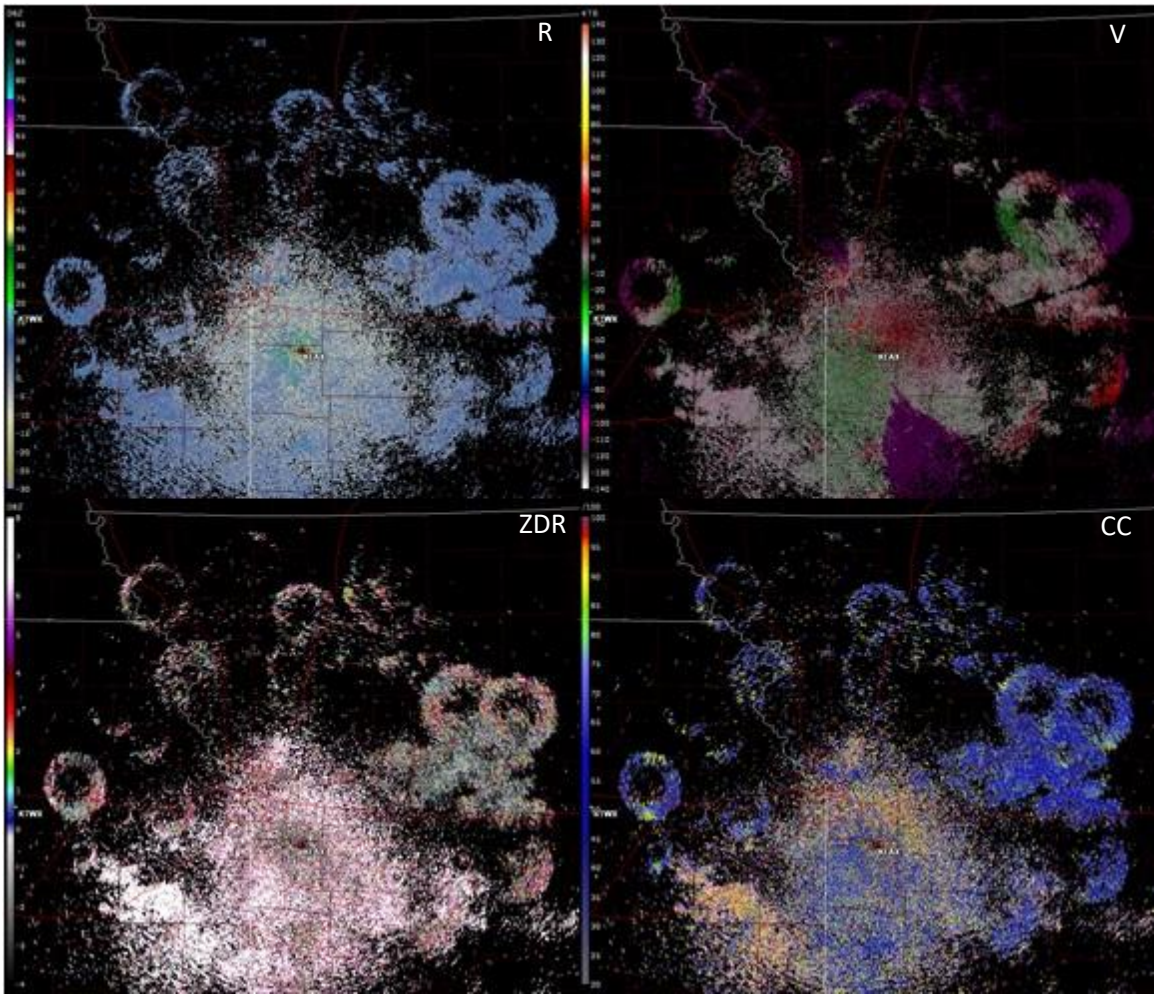

Chaff

Chaff is strips of metal foil dropped by military aircraft as a radar countermeasure and can be observed on radar products. The images below contain chaff and precipitation. Chaff has been observed since before the Dual-Pol upgrade; however, discrimination between chaff and precipitation echoes was eased due to the upgrade. Typically, radar returns from chaff have low CC and high ZDR values.

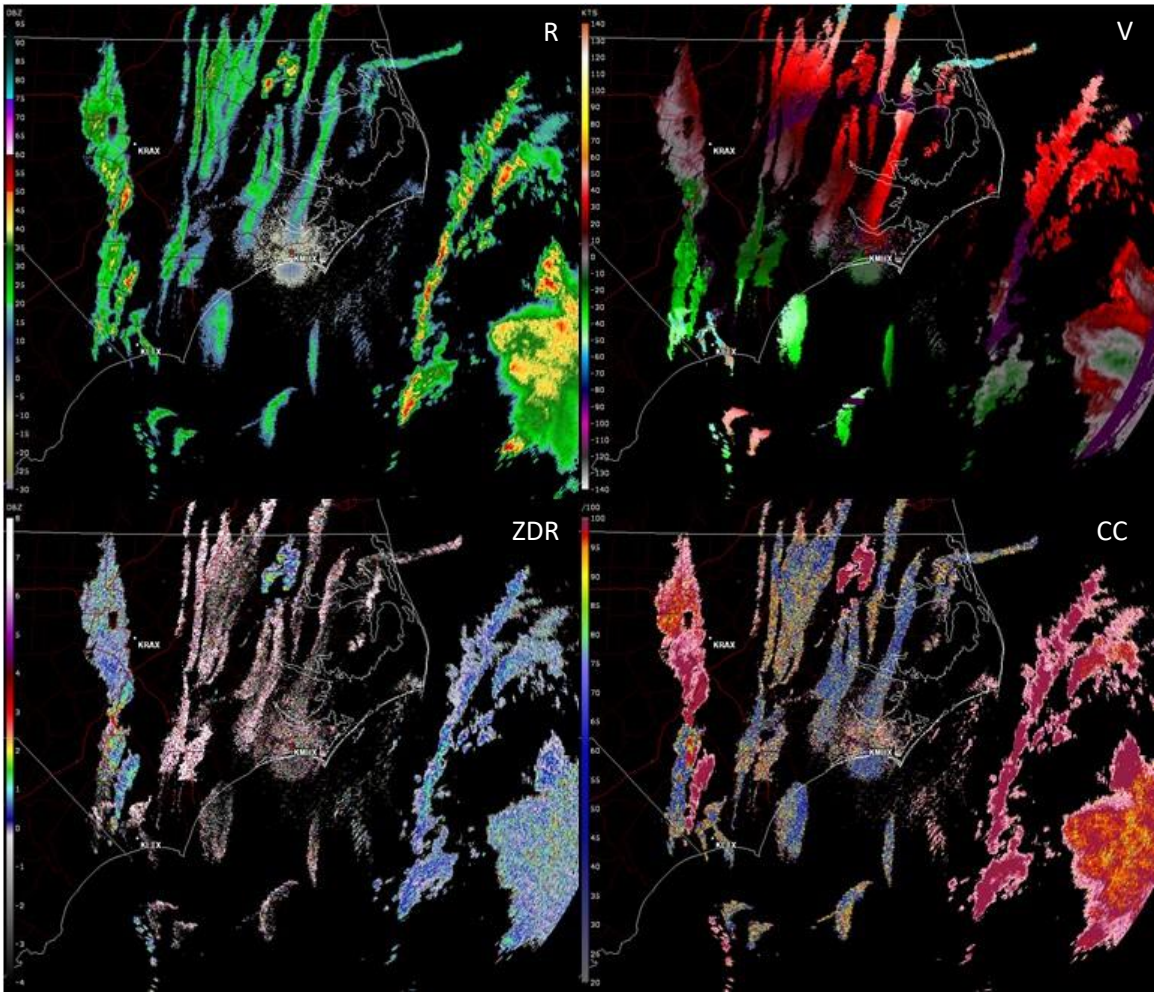

CMD False Alarms

False alarms can occur with the current version of CMD, but the number of false alarms on Split Cuts has been reduced following improvements to the algorithm. False alarms can be quite noticeable on Batch Cuts, depending on the meteorological conditions. While we are referring to theses as CMD false alarms, the underlying issue is with the Bypass Map as described in the "Data Voids from Bypass Map" issue in this document. The example below is from 1.8 degrees, which is a Batch Cut.

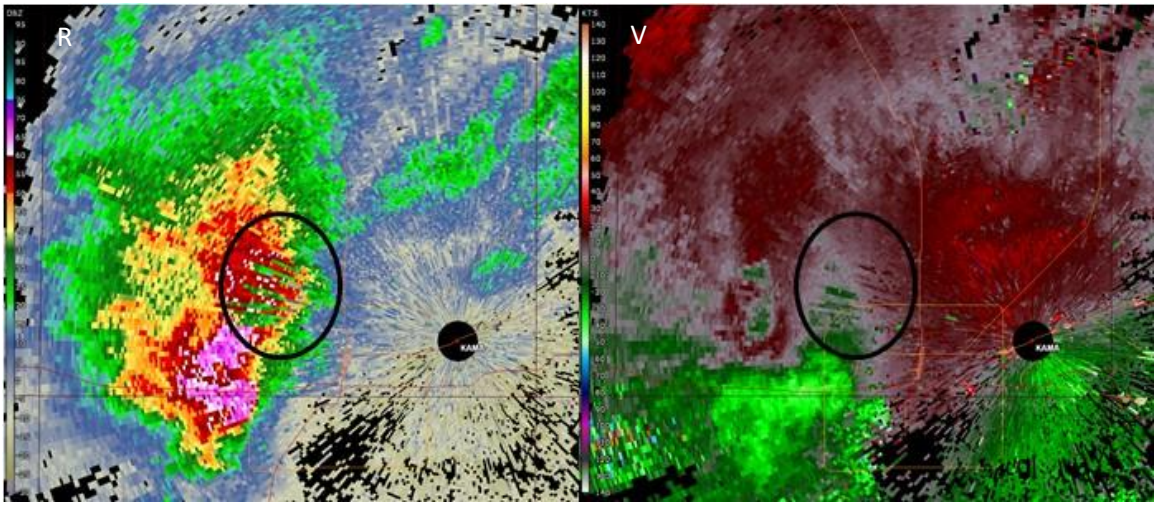

Data Voids from Bypass Map

During the first implementation of CMD, numerous field sites noticed box-shaped areas of reduced reflectivity (i.e., data voids), mainly along the zero isodop but also in areas where velocity values are a multiple of the Nyquist Interval of the Surveillance Split Cut scan. In troubleshooting, it was found that these voids have existed since pre-ORDA and are a result of the creation of the clutter bypass map. Prior to the deployment of CMD, these voids were static or stationary, which eventually became disregarded. With CMD, these data voids move from one volume to the next, depending on the bins that were flagged as containing clutter by the algorithm, catching the eye with their movement.

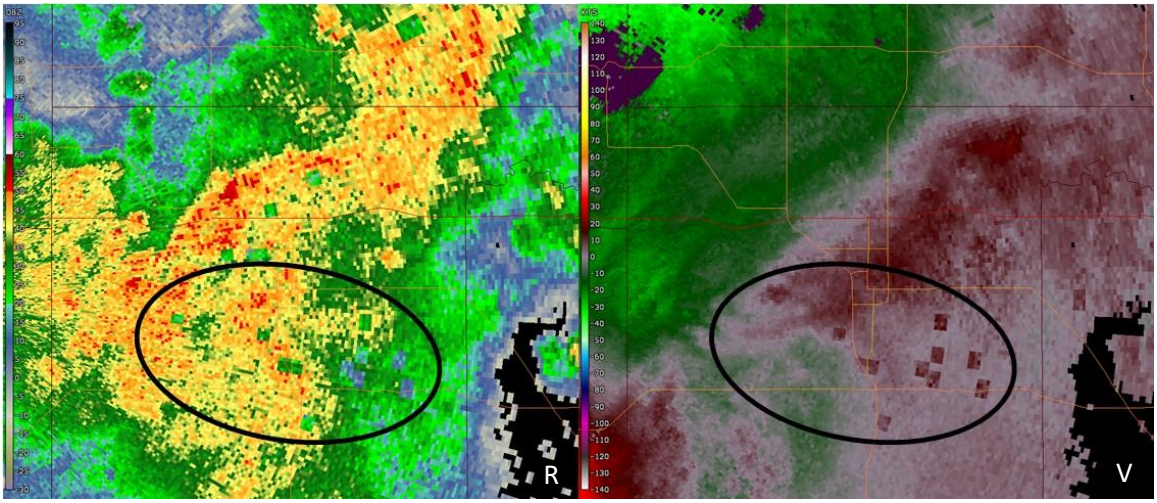

Example of reflectivity data voids along zero isodop.

Due to the way GMAP filters data, the velocity data in these areas are biased away from zero.

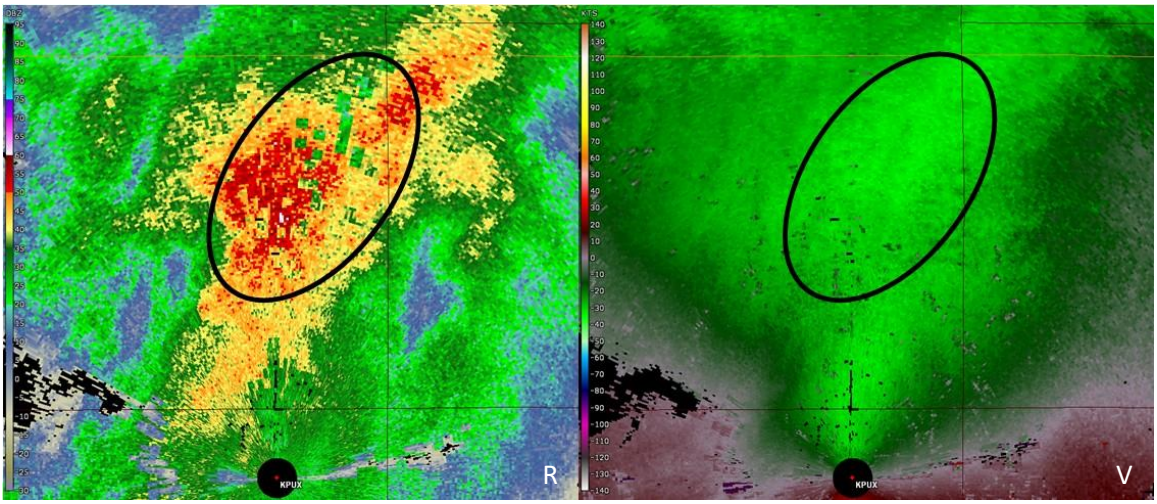

Example of reflectivity data voids for a multiple of the Nyquist.

In these cases, the impacts to velocity data are negligible.

Earthquakes

Biologicals often take flight immediately following an earthquake in their vicinity. A 4.3 earthquake occurred near Edmond, OK at 11:39 UTC on 29 December 2015 causing thousands of biologicals to take flight. The images below illustrate this phenomenon where the yellow star shows the location of the epicenter.

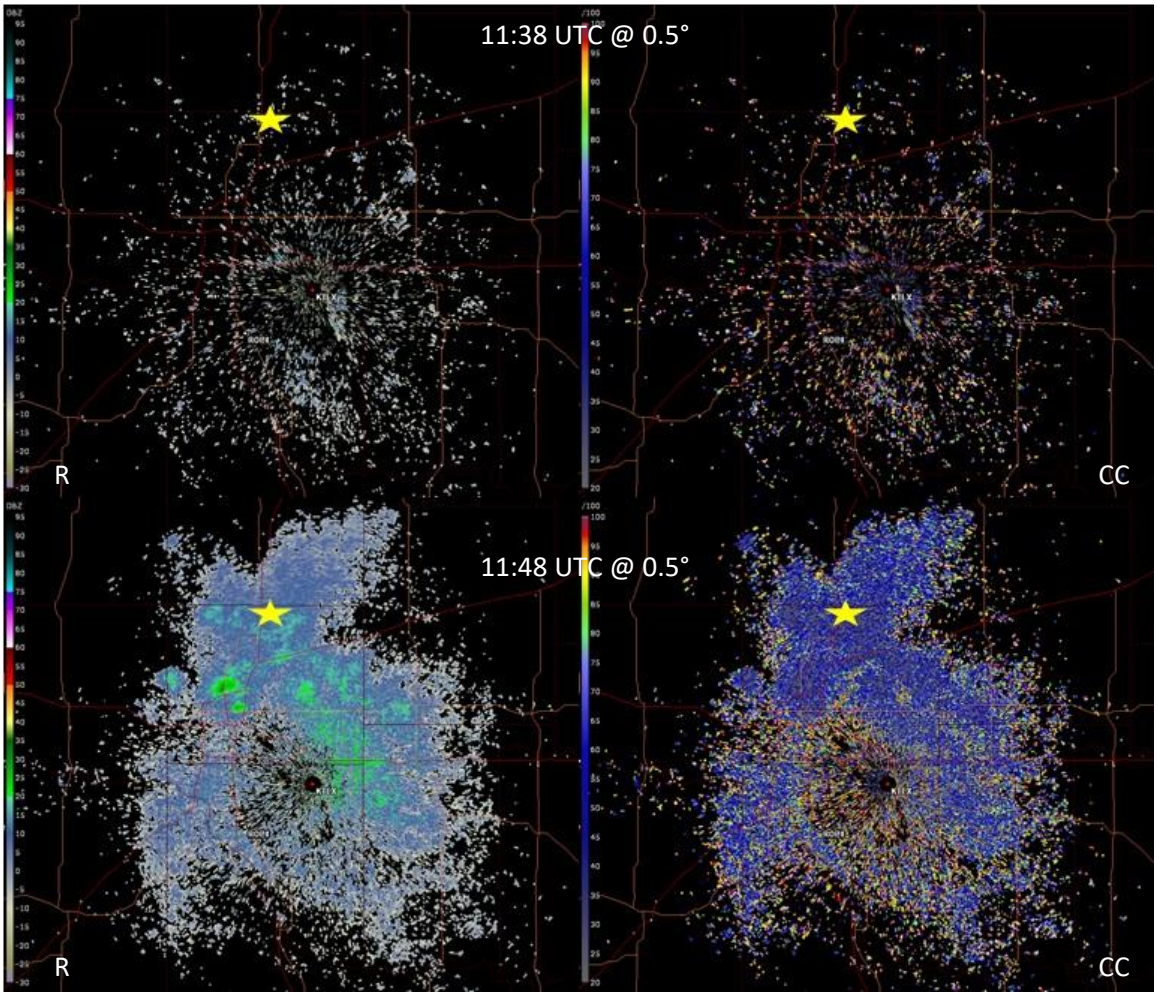

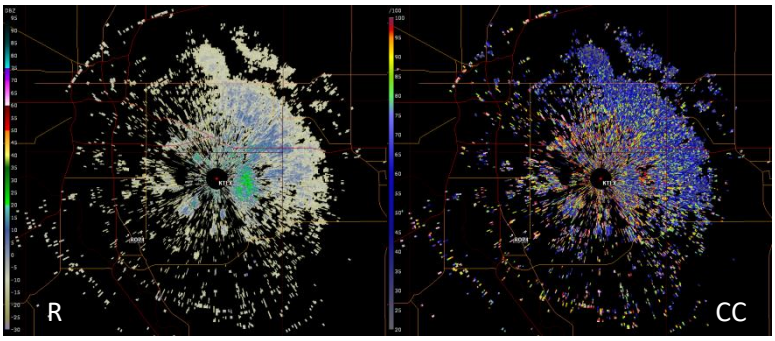

The images to the left are from 1.5°, two minutes after the earthquake.

Exclusion Zone Holes

The hybrid scan requires that the rainfall rate grid achieve a minimum percentage to be considered filled (or full). For both the PPS and QPE, this percentage is 99.9. The percentage is checked at the end of each cut. Once that percentage is reached, the hybrid scan is complete and the data (i.e., hybrid reflectivity for PPS; hybrid hydrometeor class for QPE) are sent downstream in the algorithm to be converted to rainfall estimates. If the percentage is reached before the maximum elevation angle of an exclusion zone is reached then a "no data" wedge can result.

Sites experiencing this can minimize the size of the exclusion zone, in azimuth, range, and elevation. The purpose of exclusion zones is to remove moving clutter from the precipitation accumulations – they do NOT impact base data. Exclusion zones may also be used to mitigate stationary ground clutter not always mitigated my GMAP.

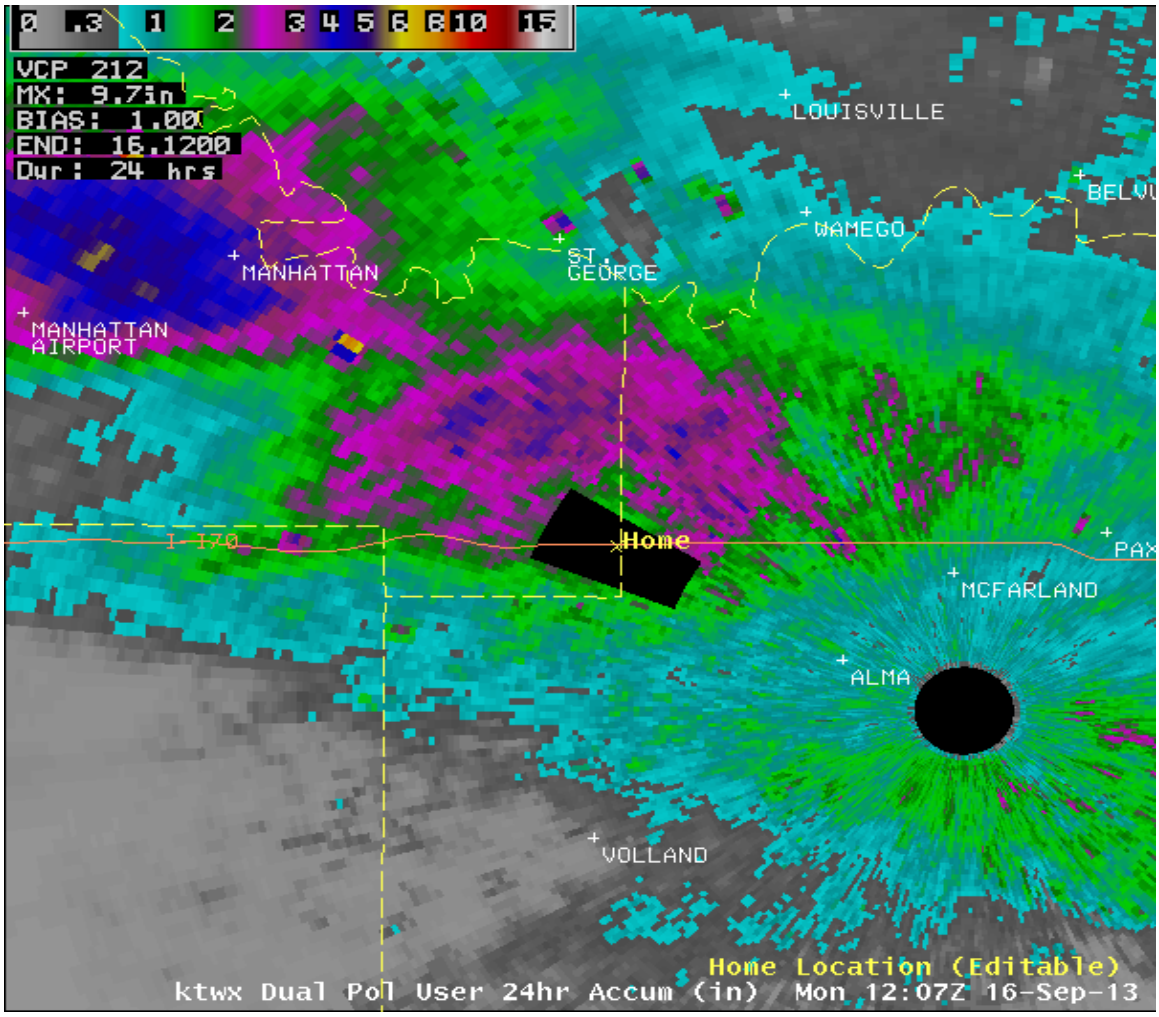

PHI Wrapping

When the initial PHI data are close to zero (i.e., 350-10 degrees), the RPG cannot properly process the data due to wrapping. Wrapping PHI data negatively impacts several Level 3 products, including ZDR, KDP, HC/HHC, and QPE. The problem can be resolved by manually updating the ISDP Adaptation Data value (i.e., st22) or accomplishing the ISDP calibration routine during appropriate conditions (i.e., light rain from 5 to 30 km from the radar). The PHI data can be evaluated in a Level 2 data viewer or in AWIPS via the raw PHI product. High PHI values have a big impact on the downstream products resulting in very high Level 3 ZDR estimates, a spoke-like appearance in KDP, erroneous HCA classifications, and low Dual-Pol precipitation estimates. In this case, the ZDR estimates in Level 2 data versus Level 3 data will often look very different, with Level 3 estimates appearing high as compared to the Level 2 estimates. Note: High Level 3 ZDR estimates do not necessarily mean an ISDP issue. Verification of Level 2 data is required. Contact the WSR-88D Hotline for assistance.

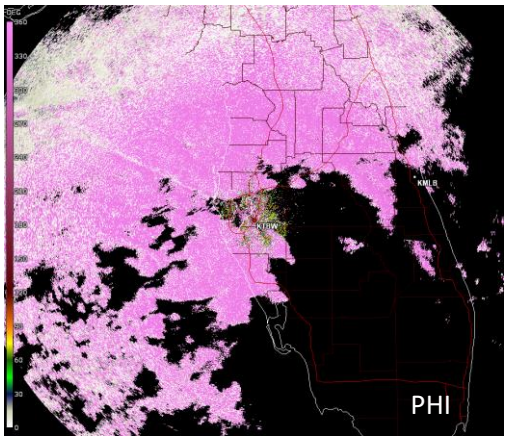

These two images illustrate PHI wrapping. The image on the left displays very high PHI values while the image on the right shows very low PHI values.

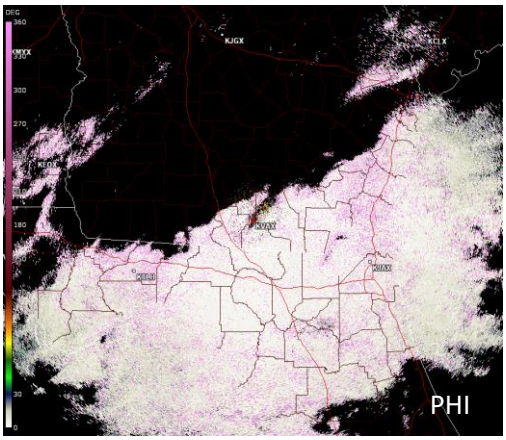

The image below illustrates the impact of high PHI values on the Level 3 ZDR.

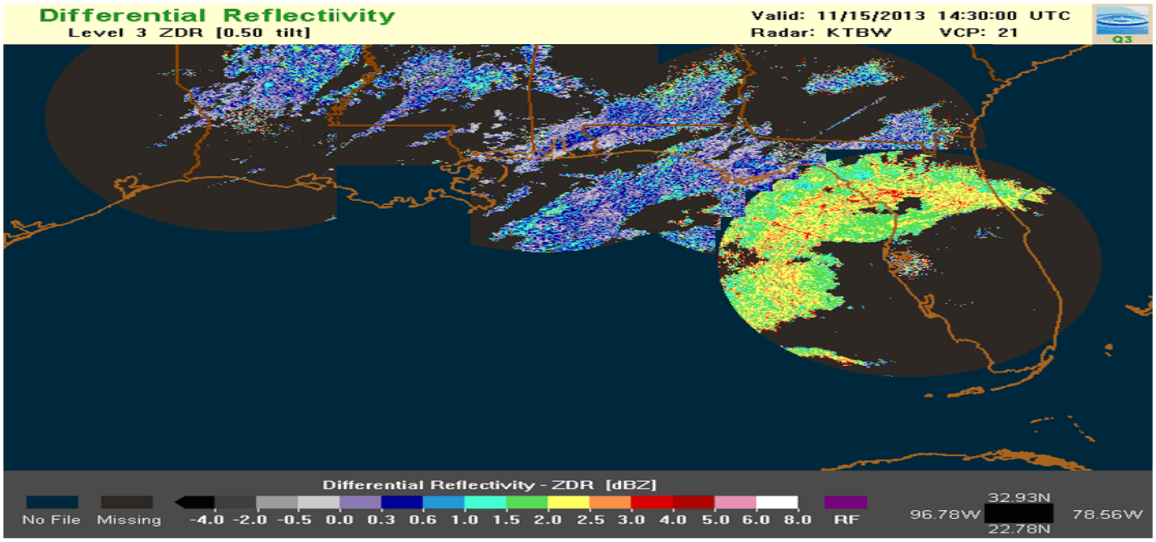

Popcorn Cities

During certain conditions, mainly occurring during the warm season, cities and towns near WSR-88D sites can be observed on the display as they “pop” up on radar. Termed “popcorn cities”, these towns show up as a cluster of returns, likely due to the heat island effect.

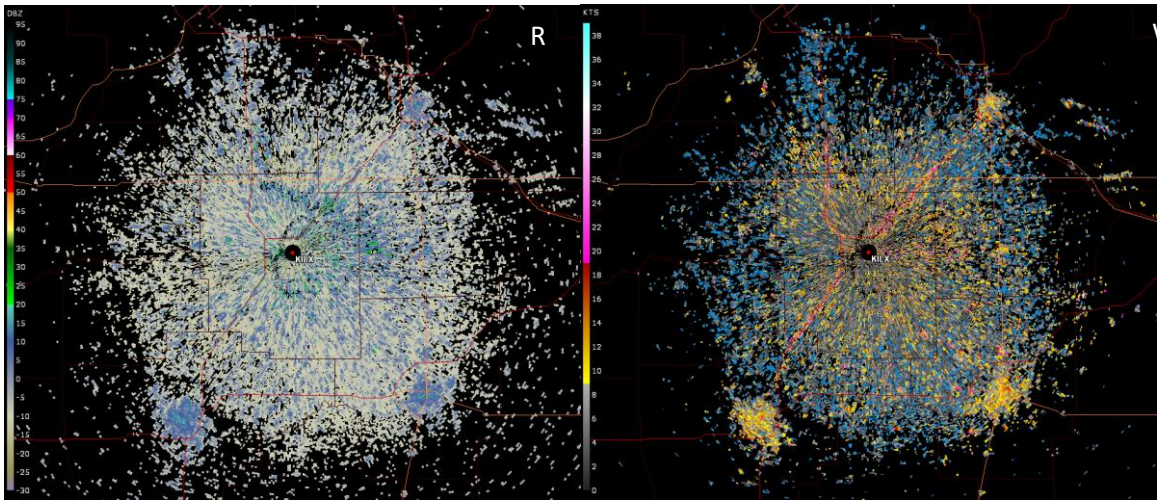

QPE Ring/Discontinuity

Rings or discontinuities may be present in QPE accumulation products. The discontinuities are collocated with the top of the melting layer. Hydrometeor classifications assigned above the top of the melting layer are dry snow and ice crystals. The rain rate relationship used for these classifications is M*R(Z), where M is some multiplier between the values of 1.0 and 2.8 and is chosen by the radar operator. The default value is 2.8 degrees, which often results in abnormally high precipitation estimates. Several rings may be observed in accumulations due to the change in the height of the melting layer throughout an event. A field test was conducted among sites in Eastern Region in order to determine a more appropriate multiplier for each participating site. These values ranged from 1.5 to 1.9 and significantly reduce the discontinuity at the top of the melting layer. Below are two images of the QPE DSA product from the same precipitation event. In the image on the left, M was set to 2.8 for both dry snow and ice crystals. In the image on the right, M was set to 1.5 for these hydrometeors.

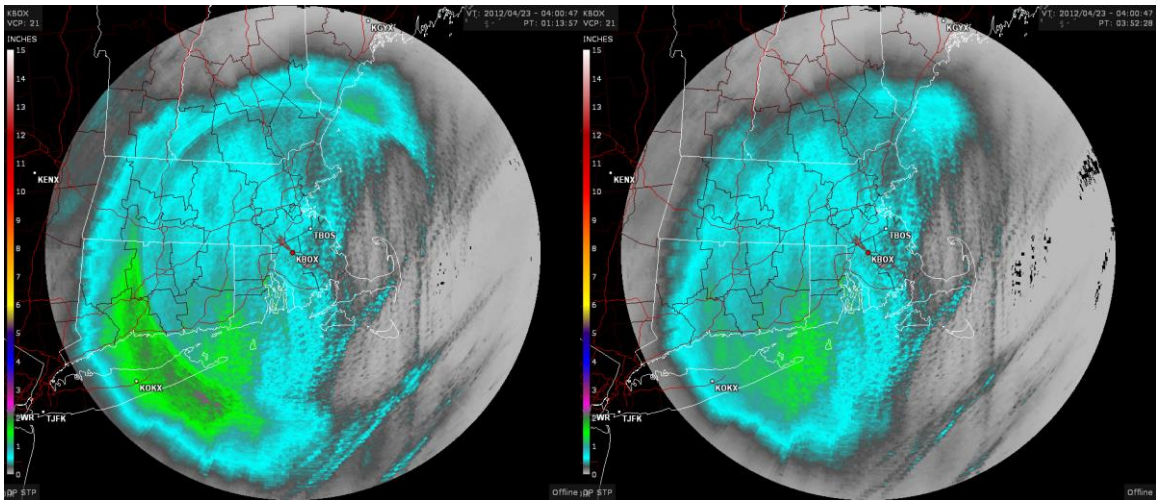

Sea Spray

Observation of sea spray is rather common on low-elevation angles from WSR-88Ds near large sources of water. The low CC values and low ZDR values indicate that the returns are from non-precipitating echoes. Evaluating R and V alone does not necessarily draw the same conclusion.

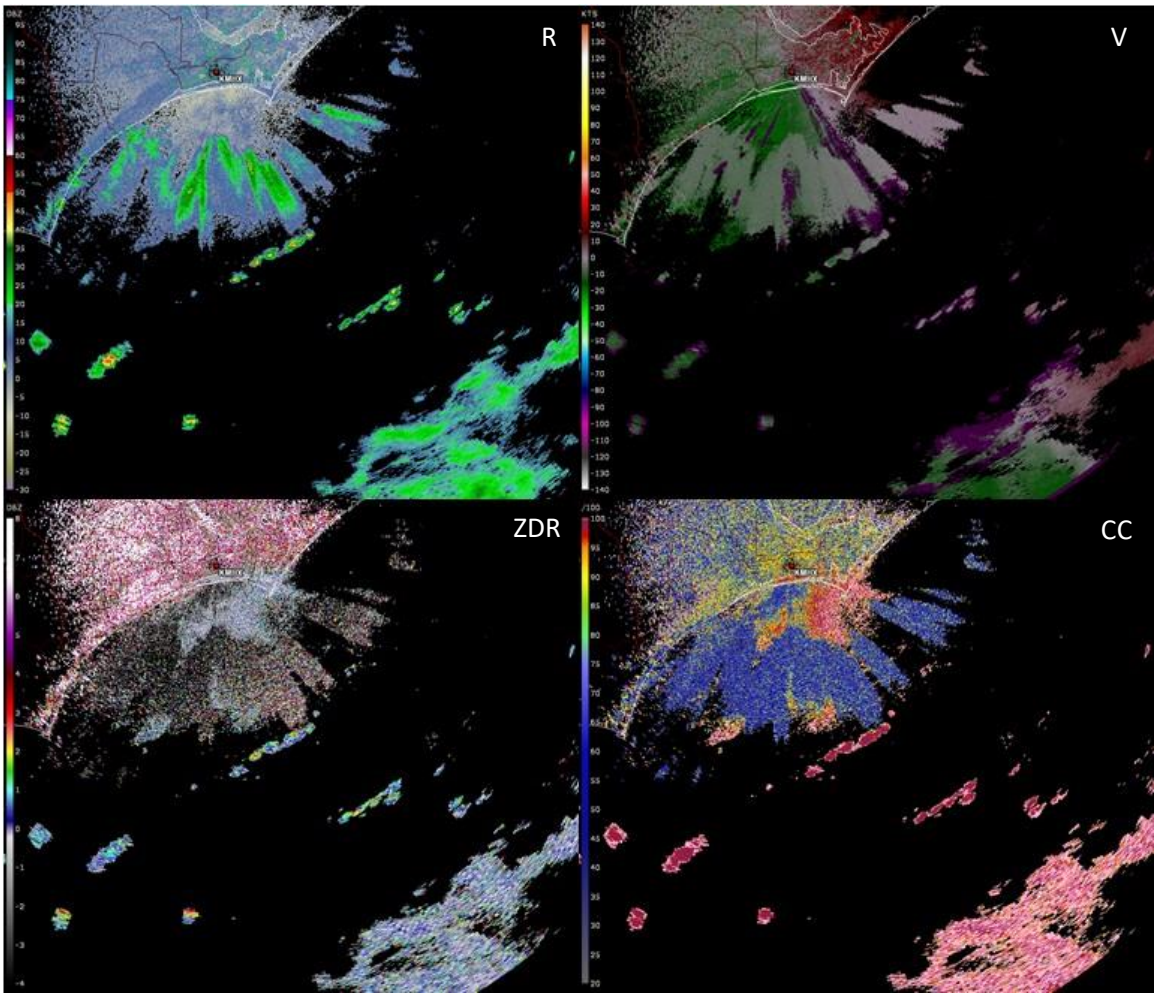

Sidelobe Contamination: Horizontal

Contamination from sidelobes can often be observed in radar data in areas of clutter, especially at sites with nearby mountains or elevated highways, in areas near storm cells, and during super refraction conditions. Proper clutter filtering can remove much of the sidelobe contamination in cases of stationary clutter. At the time of the event illustrated in the first 2-panel below, the site was running All Bins on Segment 1 and the static bypass map on all other segments. At 0.5 degrees, All Bins filtering was able to prevent the contamination from being displayed on the products while the other elevations were contaminated by sidelobes. Note: CMD was unavailable at the time of this event and will provide proper identification of this type of clutter contamination.

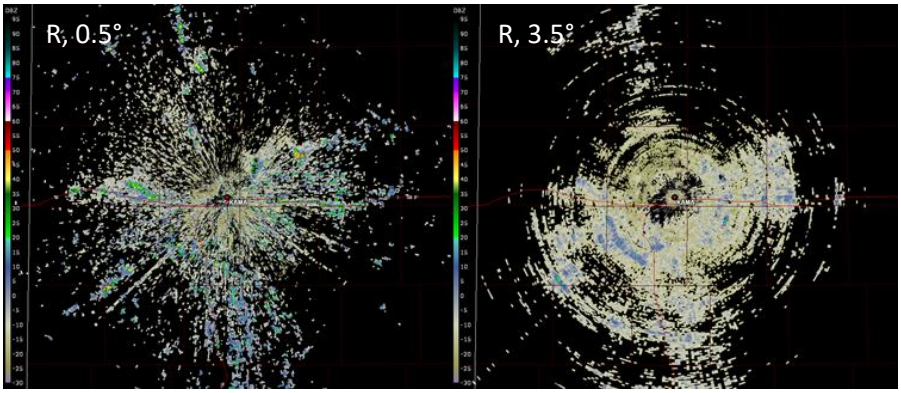

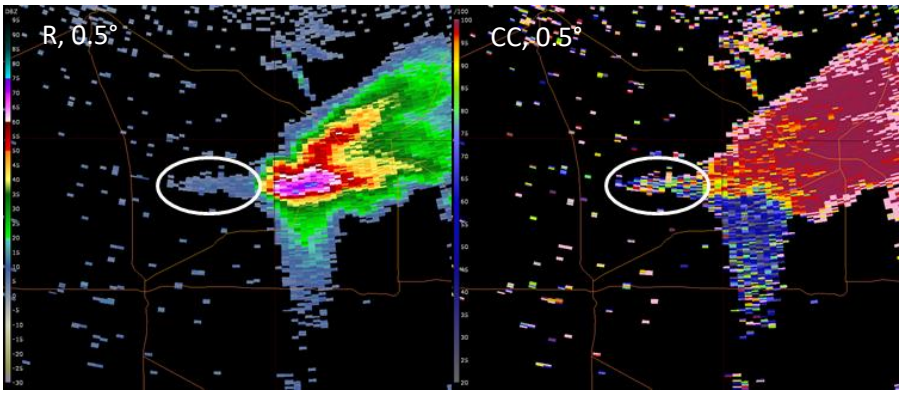

Sidelobes can contaminate data near strong storm cores, yielding a smeared appearance clockwise from the storm. Note: The larger cone-shaped smear is due to a TBSS, which is discussed in a later section of this document.

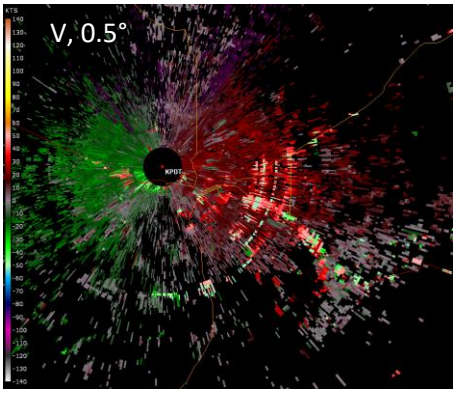

Sidelobe contamination can also manifest as small arcs as seen in the image to the left. Contamination from traffic along the highway can also be observed in the image.

Sidelobe Contamination: Vertical

Generally weak returns are received from sidelobes and the returns we see on the display are typically dominated by the mainlobe. There are rare cases, like the one illustrated below, in which the sidelobes can contaminate the data when weak return is present in the mainlobe and strong return in the sidelobes. In this example, there is weak return at 0.5 degrees but a strong rotation signature is displayed in velocity. At 2.4 degrees, a high area of reflectivity is observed with strong velocities. In comparing the data from 0.5-degrees with the data from an upper tilt, it can be concluded that the velocity was contaminated by sidelobe contamination in the vertical.

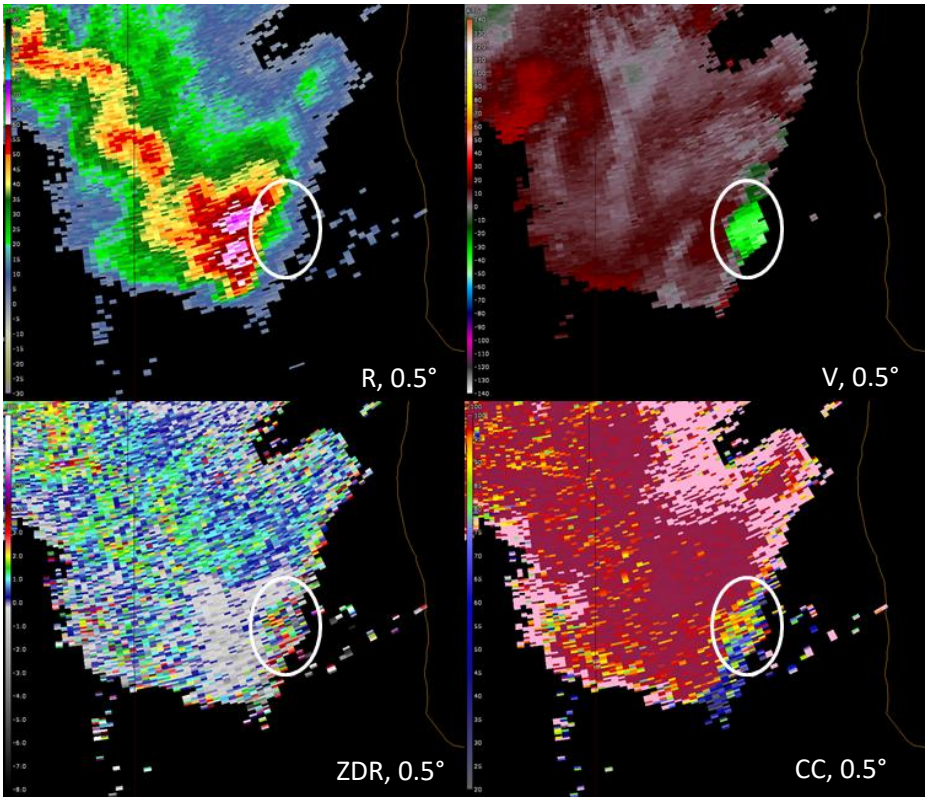

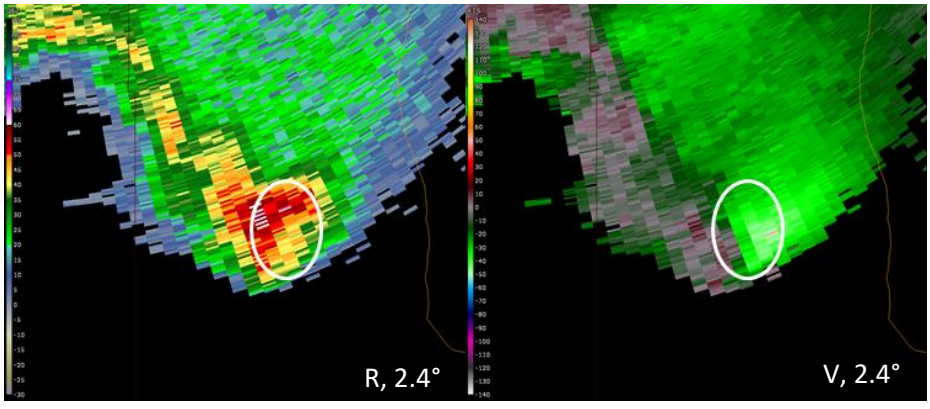

Start of Elevation Discontinuity

The start of elevation discontinuity can occasionally be observed in the data, especially when sufficient radar returns are present to allow observation of it. Often there is not a problem with the radar when this discontinuity is observed. This type of discontinuity can be due to slight elevation differences between the start and end of the elevation. Radar problems may exist if the observation is very frequent or if the antenna continues to wobble throughout the cut and VCP. Note: If the discontinuity is also observed on the Doppler Cut of a Split Cut then the observation is not due to the start of elevation.

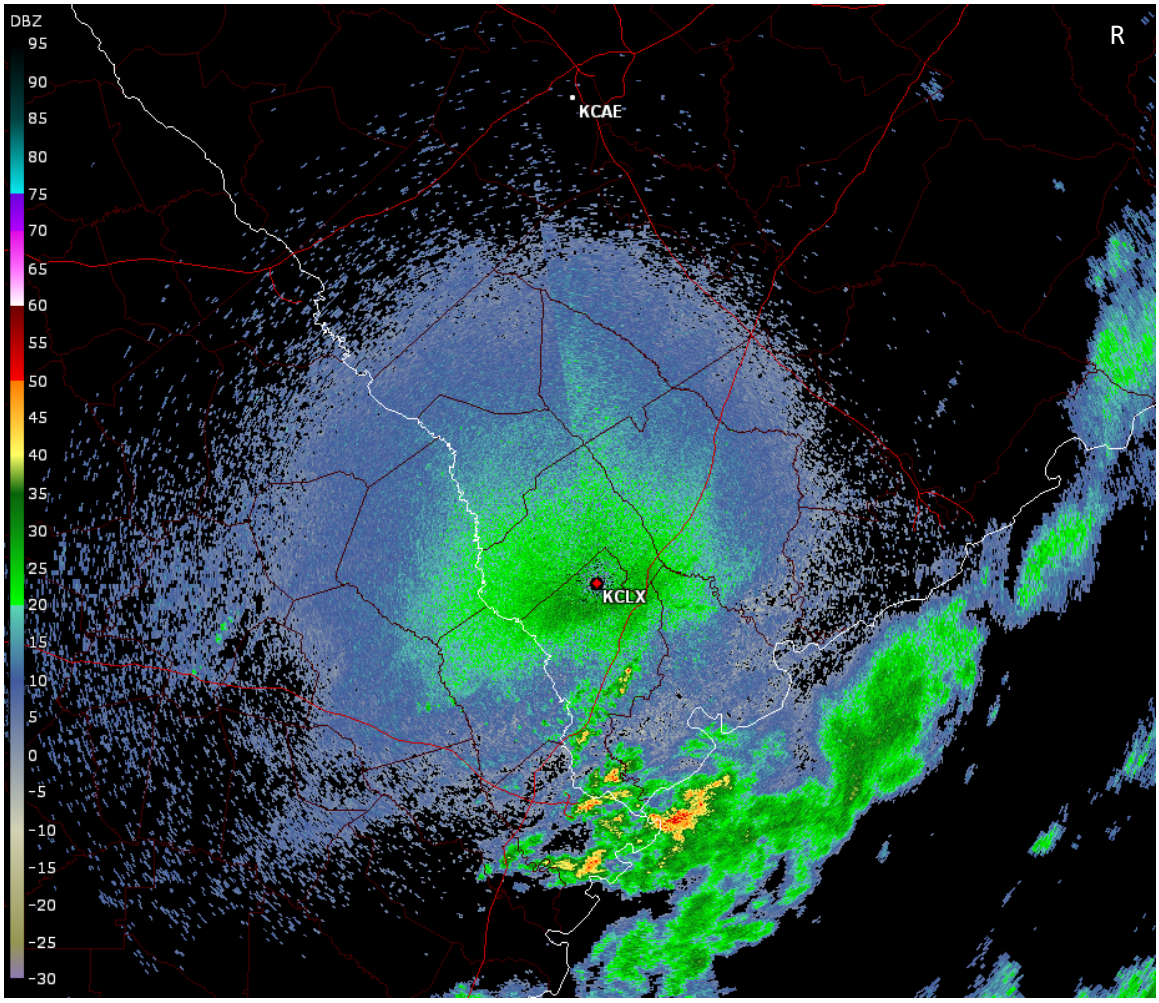

Stripes in SRM

Apparent stripes have been present in the SRM velocity product since its initialization. These discontinuities are an inherent result of mathematics used to compute storm relative motion from a velocity field. The stripes are seen more easily in a large, smooth stratiform field.

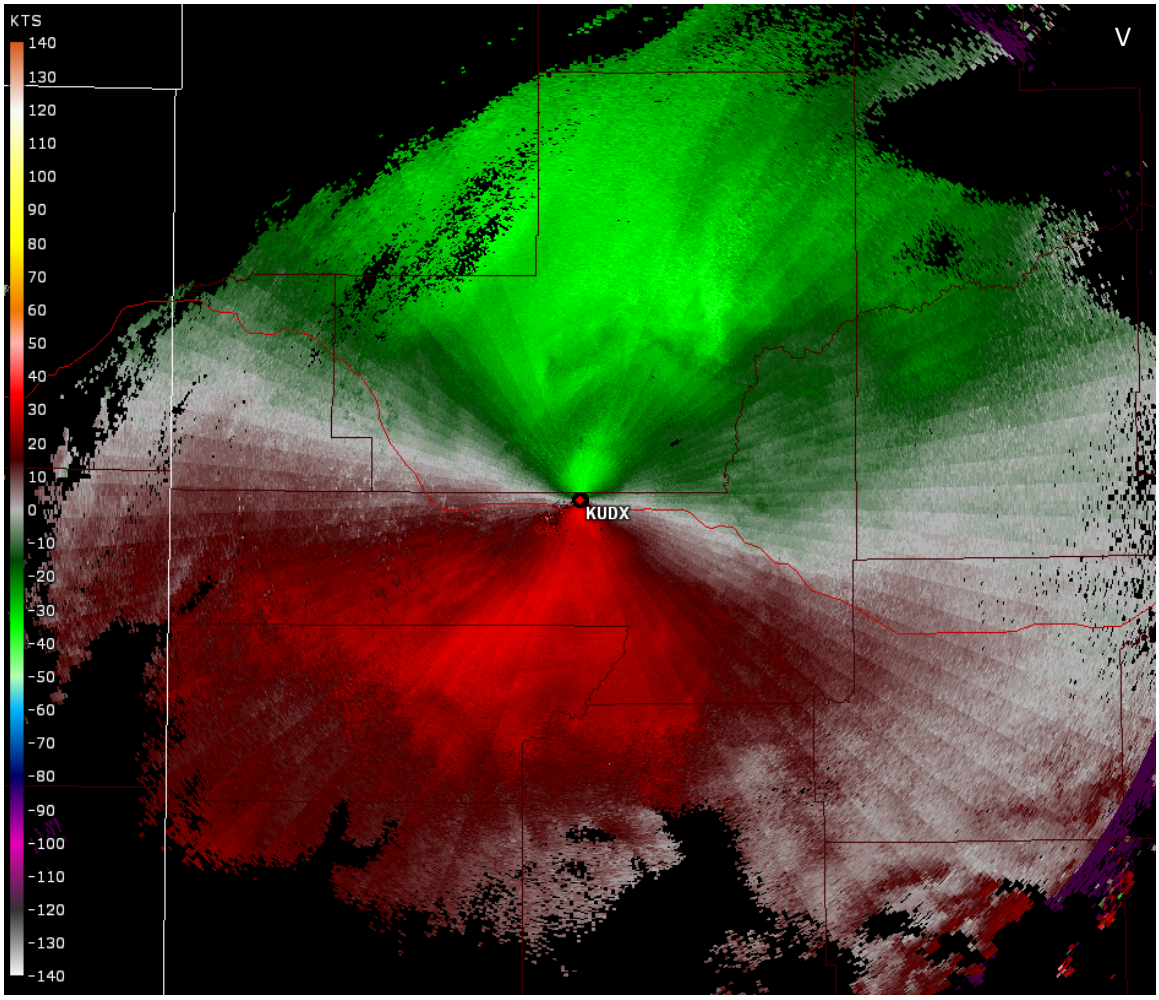

Terrain Spikes & Clutter Bursts

Terrain spikes have been observed in multiple VCPs but are often most apparent in VCPs 12 and 212. As the name implies, terrain spikes are radials of anomalous reflectivity that span across hills and mountains. These have been observed for several builds and regardless of the clutter map in place. In other words, terrain spikes continue to exist when forced filtering (i.e., all bins) is applied to the data. Occasionally, these same areas of clutter can increase or 'burst'. This anomaly is referred to as clutter bursts. Weather signal intensities do not increase during these bursts of clutter. No fix has been provided for these issues.

Terrain Spikes

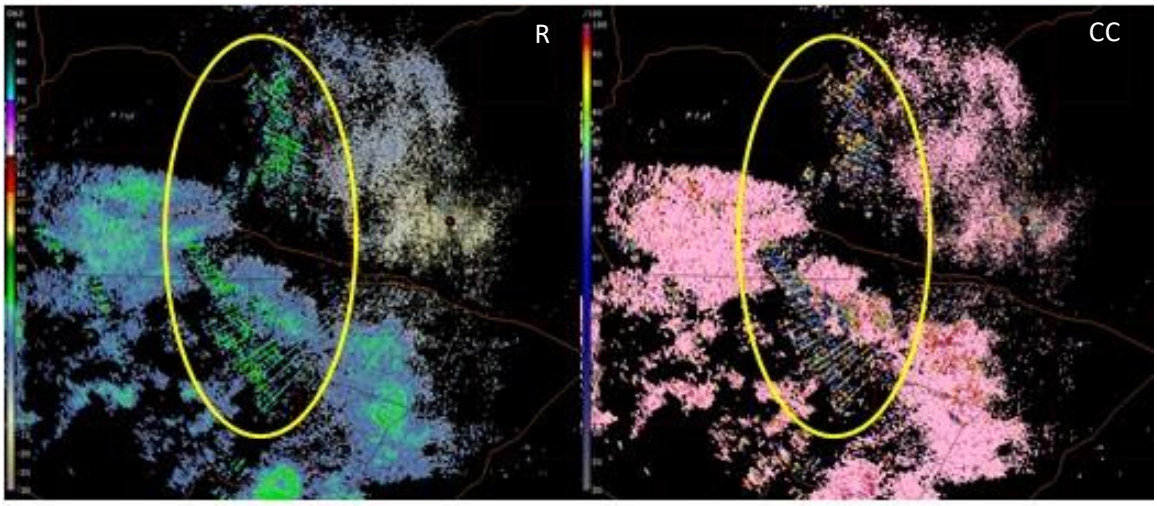

Clutter Burst

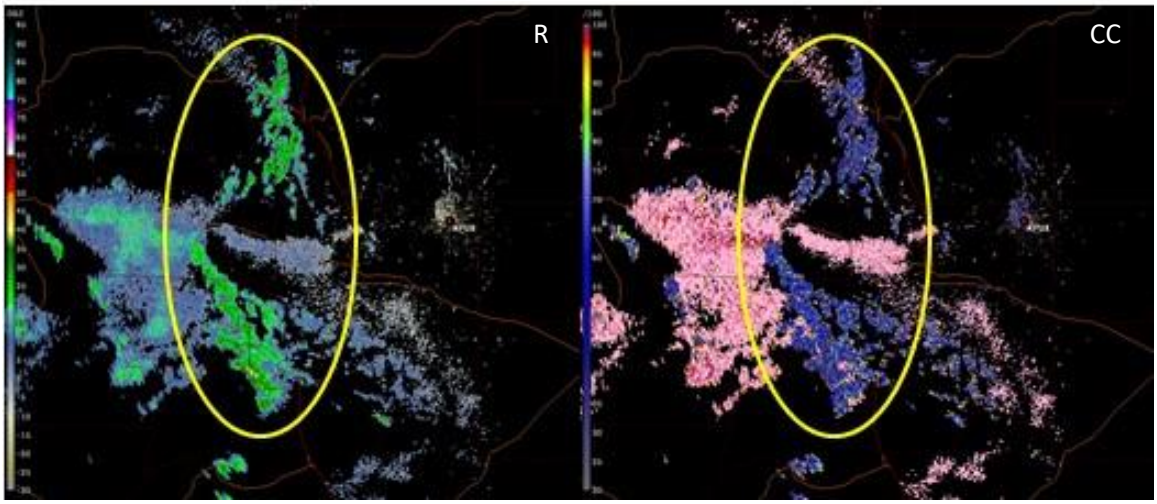

Three Body Scatter Spike

The phenomenon known as a Three Body Scatter Spike (TBSS) is the result of the radar beam passing through an area of high reflectivity. Within this area, the beam bounces off large hydrometeors, mostly large wet hail, which is subsequently deflected to the ground and back up into the storm before returning to the RDA. This produces a false radar echo that extends down radial from the storm. The spike can be seen not only in the reflectivity data but also in the CC data. The low CC values associated with this feature make it quite obvious.

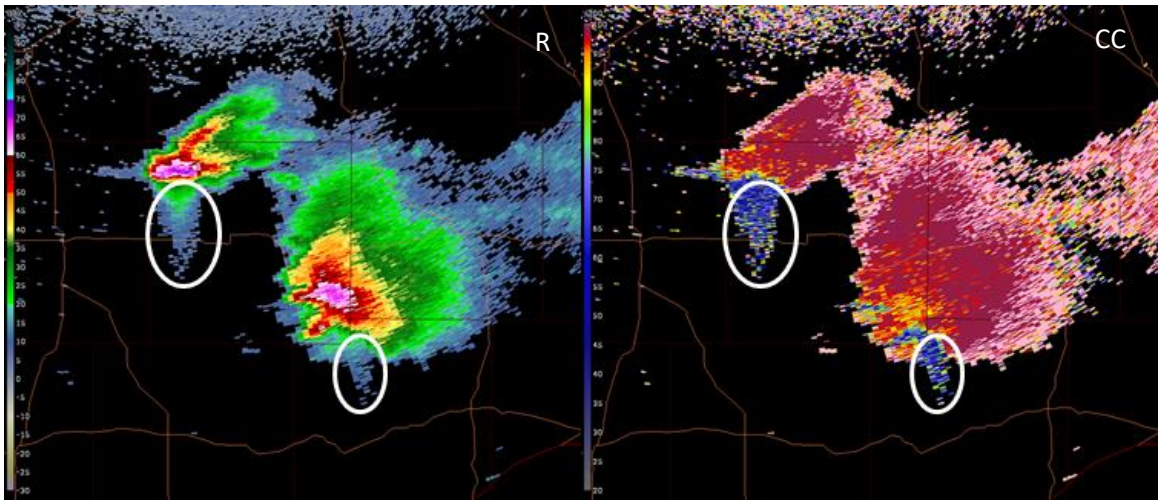

Velocity Dealiasing Errors: VCP 31

Due to a small Nyquist interval, VCP 31 is susceptible to velocity dealiasing errors. The first example below is a comparison of VCP 31 (left) and VCP 32 (right). The errors in VCP 31 can have different visual characteristics, such as the example at bottom. Although 2D-VDA (2-D Velocity Dealiasing Algorithm) helps to mitigate the errors in VCP 31, errors can still occur. It should be noted that although VCP 31 is susceptible to velocity dealiasing errors it is a useful VCP, especially during light stratiform rain or snow as it does have the best sensitivity of currently available VCPs.

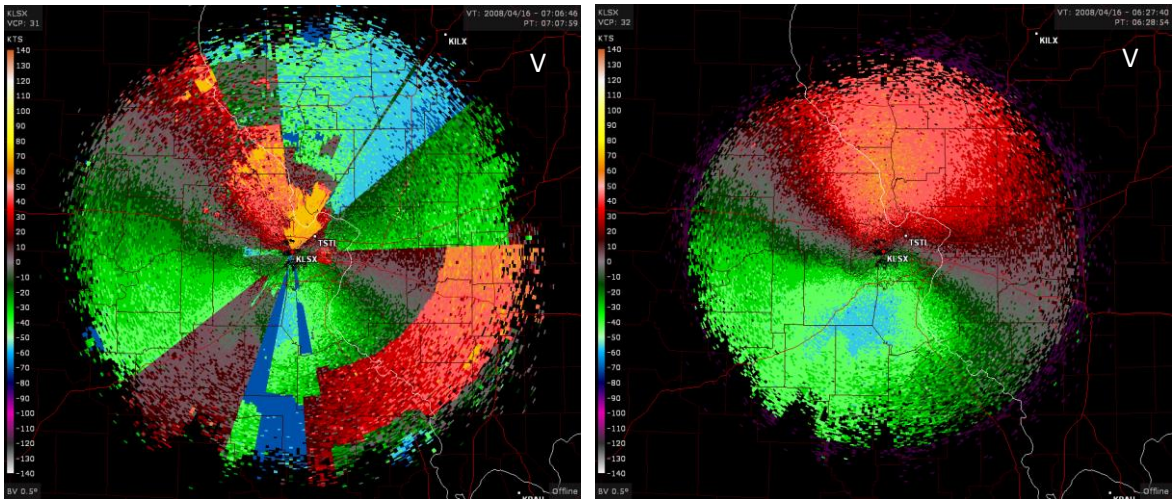

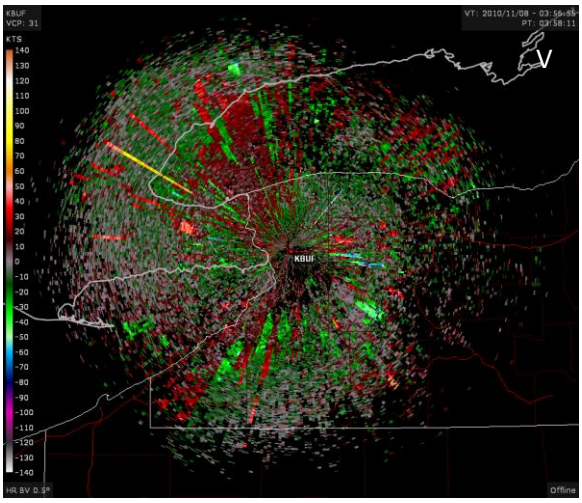

Velocity Dealiasing Errors

The following images illustrate examples of dealiasing errors from both dealiasing algorithms: the VDA and the 2D-VDA.

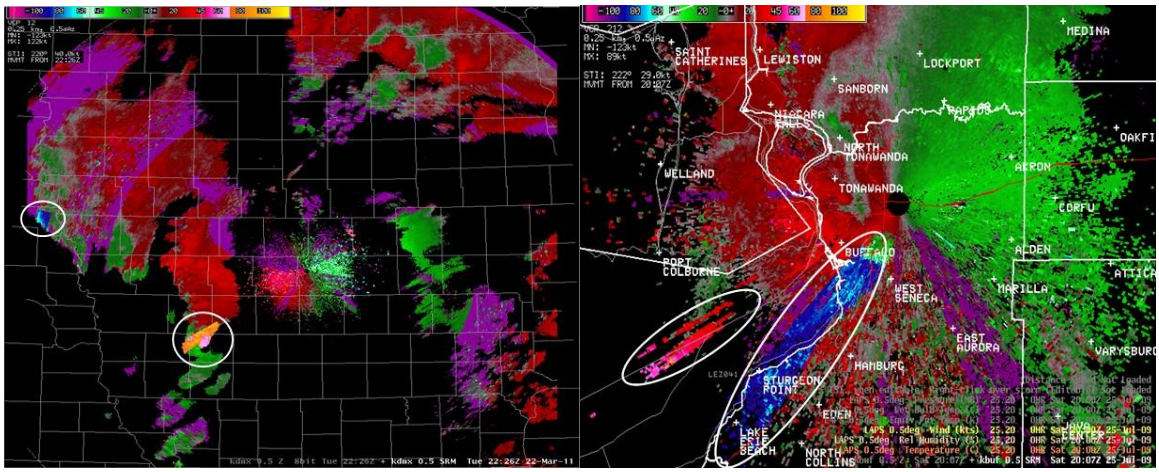

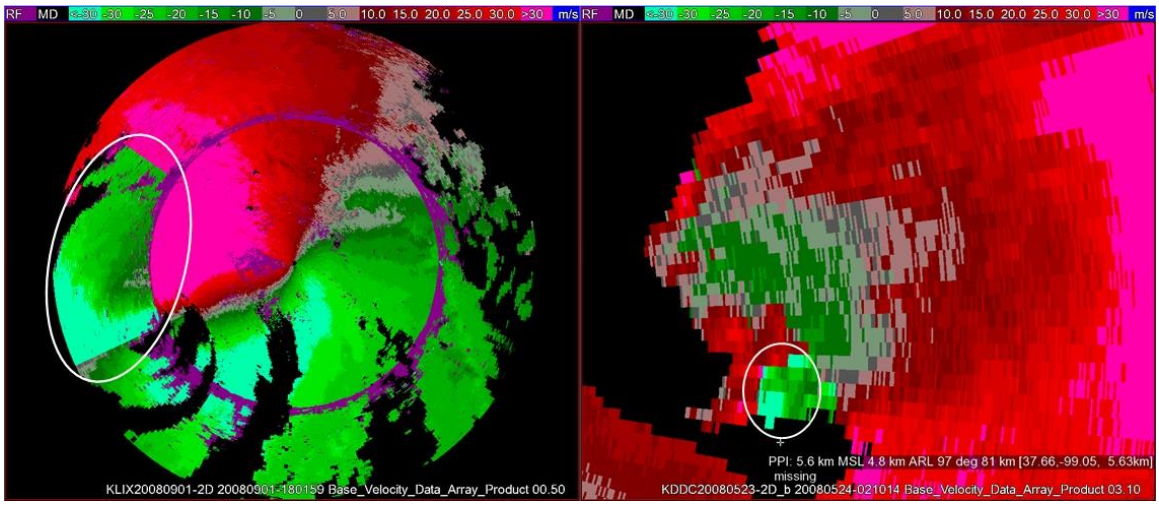

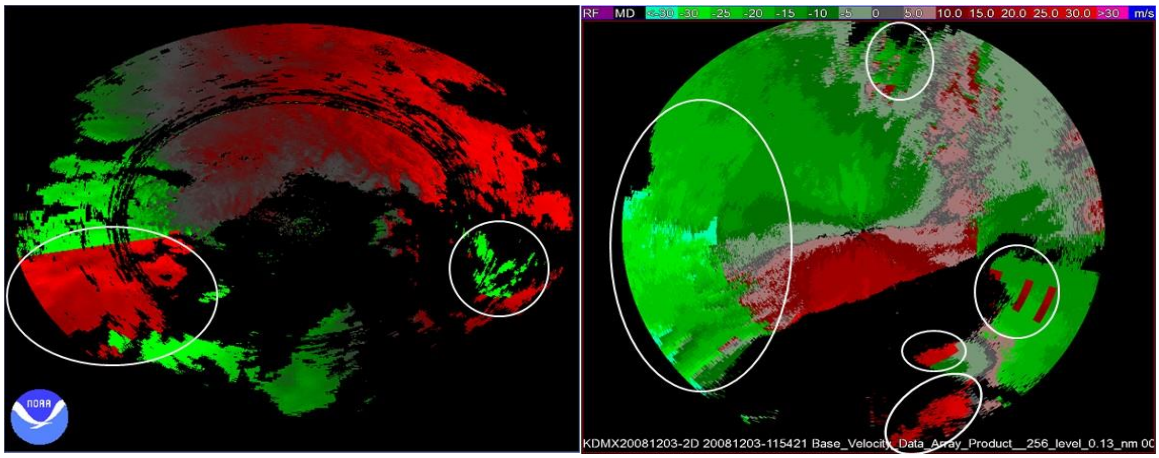

Wet Radome Effect

We are already familiar with the effect attenuation has on reflectivity. During an event, while precipitation is over the radome, there may be a couple of volumes in which the reflectivity estimates are lower than during the rest of the loop. The opposite observation may be seen in the ZDR estimates. It is theorized that as the precipitation forms rivulets along the side of the radome, the effect of attenuation is greater in the vertical than the horizontal causing a brief enhancement (or blossom) in the ZDR estimates. The examples below illustrate a wet radome effect with the images on the right showing the result of attenuation.

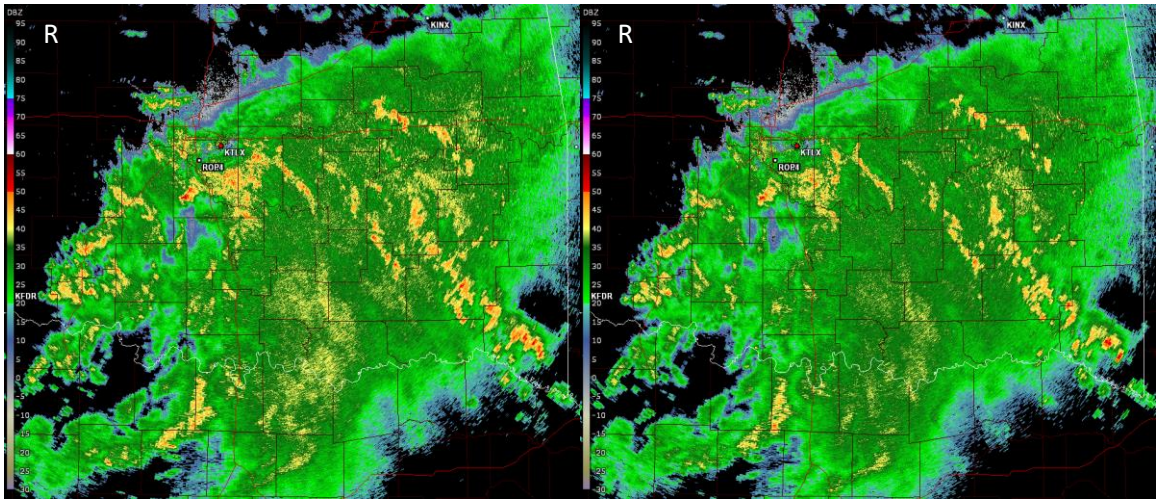

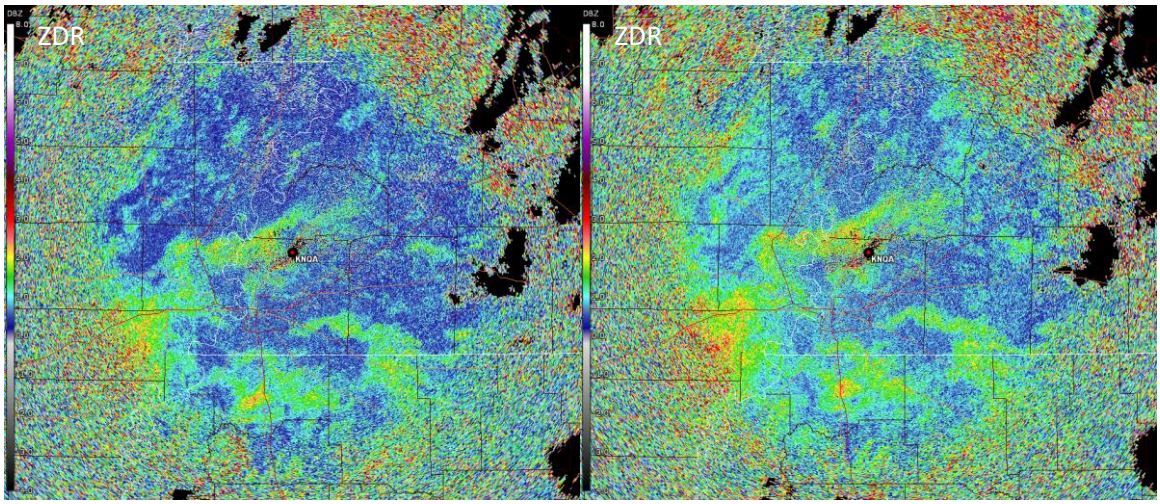

ZDR Wedges/Spikes

There are many reasons why we might see wedges (or spikes) of relatively higher, or lower, ZDR estimates. Some of these reasons are natural. There may be trees, cell towers, water towers, etc. that block the beam more in the vertical than the horizontal. This would lead to a wedge of increased ZDR estimates down range along the radial(s) from where the blockage exists. We have also seen differential attenuation due to strong reflectivity cores, which results in lower ZDR estimates down radial from the storm core.

Other examples of wedges of erroneous ZDR estimates have been a result of hardware issues, including loose cables. Some of the hardware issues have also resulted in rotating wedges of erroneous ZDR estimates or even wedges of no data. These wedges have shown higher and lower ZDR estimates and can be observed in both Level 2 and Level 3 data. The Specific Attenuation R(A) QPE rate method, introduced in RPG Build 19.0, mitigates the effect of partial beam blockage below the melting layer. Hardware-related issues, however, must be resolved by site personnel—ROC assistance is available, as needed. Each ZDR wedge case is different and must be investigated in order to determine the cause.

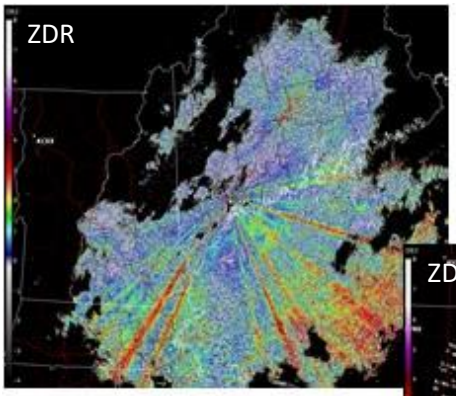

Example of ZDR wedges due to partial beam blockages.

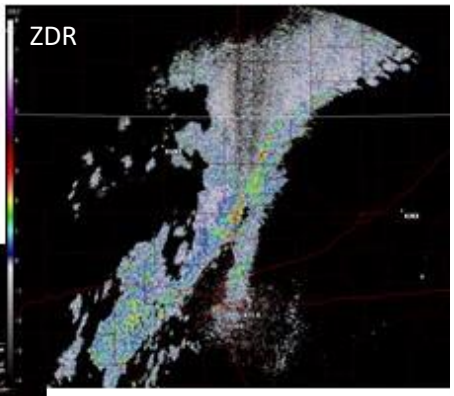

Example of ZDR wedges due to differential attenuation.

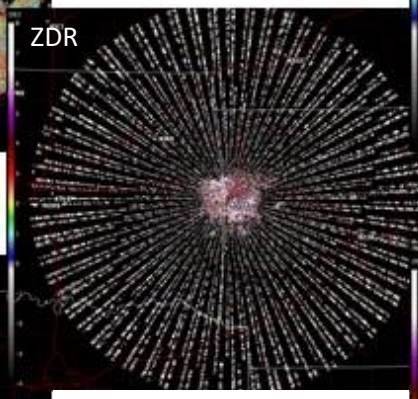

Example of ZDR spikes due to hardware issues.

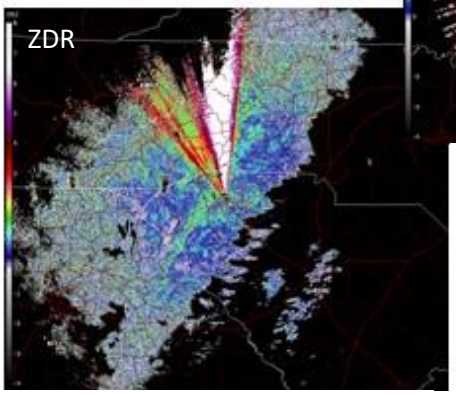

Example of ZDR wedges due to hardware issues. In this case, the wedge was resolved with R&R of the Azimuth Rotary Joint.

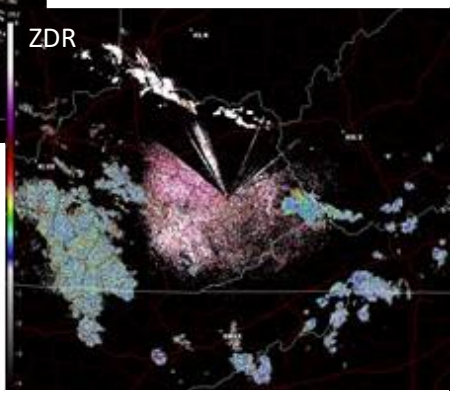

Example of ZDR wedges due to hardware issues. In this case, the wedges were resolved by tightening the cables connecting one of the LNAs.

Past Topics:

Clutter Footprint

Formerly, CMD was not very efficient at identifying areas of weak clutter. Although all Dual-Pol variables are susceptible to the effects of missed clutter detections, Correlation Coefficient is particularly sensitive to clutter residue. The effects on the CC product have been termed "Clutter Footprint". Improvements were made to the CMD algorithm in RDA Build 18.2 which significantly reduces the Clutter Footprint issue in the Dual Pol variables. Note that this change does not affect the legacy base data (i.e., R, V, and W). Below is an example of the same volume of data with and without the improvements deployed in RDA Build 18.2.

CC before the RDA Build 18.2 Improvements

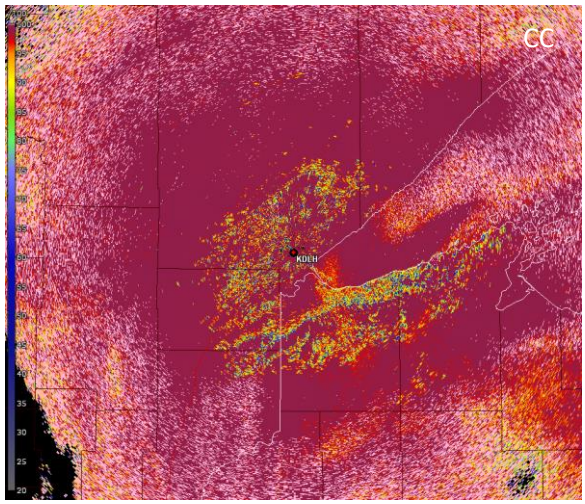

CC with the RDA Build 18.2 Improvements

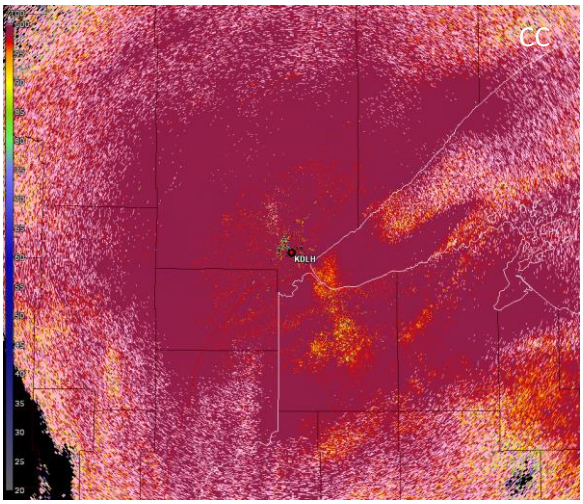

Corresponding reflectivity image

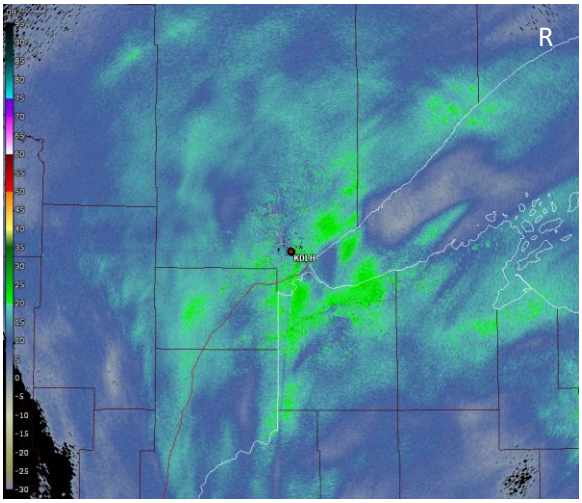

PHI Initial Target Value

Prior to RDA Build 14.0, the initial target value for PHI estimates was 25 degrees. Starting with RDA Build 14.0, however, the target value changed to 60 degrees. The goal of this change is to mitigate how often the ISDP calibration needs to be completed. Tweaks to hardware (i.e., cables) and changes in ambient temperature can result in shifts or drifts in the initial value. Repeated drifts can result in the PHI Wrapping issue discussed in this document. A new color table has been developed for the new target so the color of 60 degrees is blue. If using the original color table for PHI (with Build 14) then one would expect dark green. Below is an example of the same volume of data processed from RDA Build 14. The image on the left is displayed with the original color table while the image on the right is displayed with the adjusted table so that we see blue, as accustomed. Note: The initial PHI value is estimated at the edge of precipitation nearest the radar.

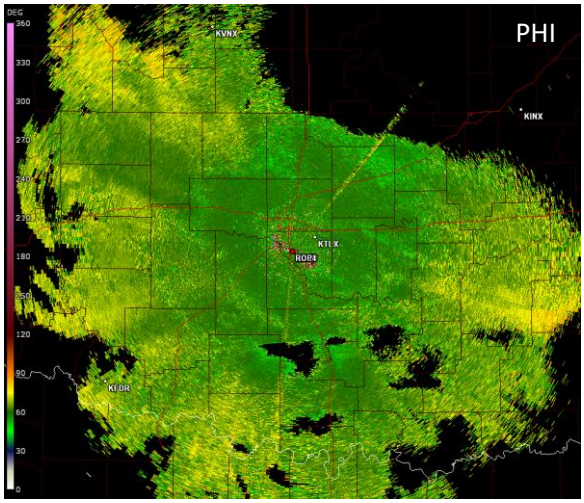

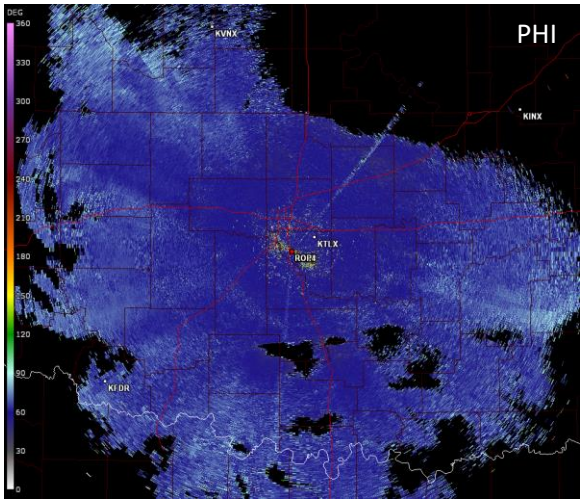

Radial Spikes of Zero Knots in Spectrum Width

Observations of radially-oriented spikes of zero knots in Spectrum Width products were documented in previous software builds. These spikes were observed ***only*** in Batch Cuts of VCP 32 when PRF 8 was active.

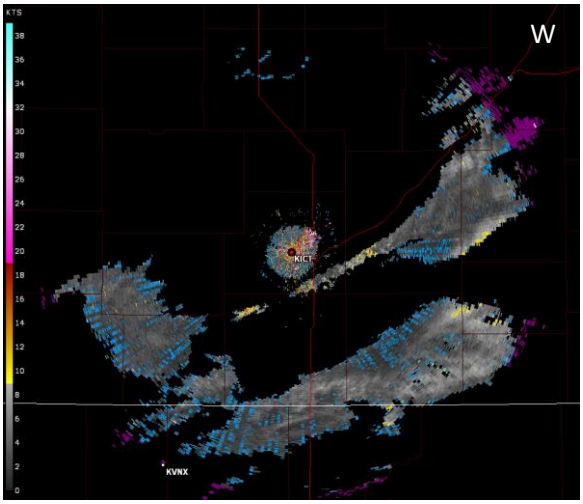

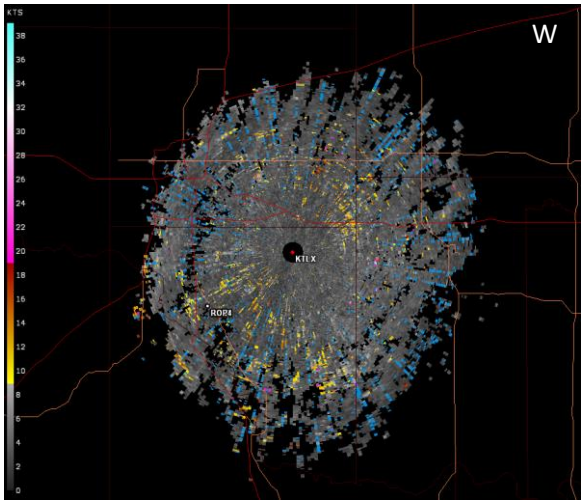

Shimmy

The "shimmy" was discovered when Super Resolution data became available; although, the problem had existed for numerous builds. The "shimmy" was an apparent shift in the radar data which could be observed when switching from a clear air VCP to a precipitation VCP and vice versa. Examples from the field have been documented in the WSR-88D Field Support Hotline. The cause of this issue was due to latency between the DCU and the RCP8/RVP8 and was fixed in Builds 10.3 and 11. As a side note, the DCU became obsolete with the introduction of the Radar Signal Processor in Build 17.

SZ-2 in Manual PRF Bug

In Build 16.0, SZ-2 PRF selection was introduced. This change also introduced a bug. For manual PRF selection, the RPG HCI failed to change the scan rate for SZ-2 cut when the operator changed the PRF value. When this occurred, the RPG received numerous "Number of Recomb Rads in Cut > 400 → Forced End of El/Vol" messages, which often resulted in wedges of "no data" on many Level 3 products. This issue was fixed in Build 18.

Acronyms

2D-VDA	Two-Dimensional Velocity Dealiasing Algorithm
AWIPS	Advance Weather Interactive Processing System
CC	Correlation Coefficient
CMD	Clutter Mitigation Decision
dBZ	Decibel Relative to Reflectivity
DHR	Digital Hybrid Reflectivity
DoD	Department of Defense
DSP	PPS Digital Storm Total Precipitation
DSA	QPE Digital Storm Total Accumulation
FAA	Federal Aviation Administration
GMAP	Gaussian Model Adaptive Processing
HCA	Hydrometeor Classification Algorithm
HC	Hydrometeor Classification
HHC	Hybrid Hydrometeor Classification
HSR	Hybrid Scan Reflectivity
ISDP	Initial System Differential Phase
KDP	Specific Differential Phase
LNA	Low Noise Amplifier
PHI	Differential Phase
PPS	Precipitation Processing Subsystem
PRF	Pulse Repetition Frequency
QPE	Quantitative Precipitation Estimation
R	Reflectivity
R&R	Removal and Replacement
RDA	Radar Data Acquisition
ROC	Radar Operations Center
RPG	Radar Product Generator
SRM	Storm Relative Motion
STA	QPE Storm Total Accumulation
SW or W	Spectrum Width
SZ-2	Sachidananda-Zrnić Phase Coding
TBSS	Three Body Scatter Spike
UTC	Coordinated Universal Time
V	Velocity
VCP	Volume Coverage Pattern
VDA	Velocity Dealiasing Algorithm
WSR-88D	Weather Surveillance Radar-1988 Doppler
ZDR	Differential Reflectivity